

# Spatio-temporal variability of phytoplankton assemblages and its controlling factors in spring and summer in the Subei Shoal of Yellow Sea, China

Yuanzi Huo<sup>1,2\*</sup>, Honghua Shi<sup>3</sup>, Jianheng Zhang<sup>1</sup>, Qiao Liu<sup>1</sup>, Yuanliang Duan<sup>1</sup>, Qing He<sup>1</sup>, Kefeng Yu<sup>1</sup>, Hongsheng Bi<sup>2</sup>, Chunlei Fan<sup>4</sup>, Peimin He<sup>1</sup>

<sup>1</sup> College of Marine Ecology and Environment, Shanghai Ocean University, Shanghai 201306, China

<sup>2</sup> Chesapeake Biological Laboratory, University of Maryland Center for Environmental Science, Solomons, MD 20688, USA

<sup>3</sup> First Institute of Oceanography, Ministry of Natural Resources, Qingdao 266061, China

<sup>4</sup> Biology Department, Patuxent Environmental & Aquatic Research Laboratory, Morgan State University, Saint Leonard, MD 20685, USA

Received 21 June 2018; accepted 20 August 2018

© Chinese Society for Oceanography and Springer-Verlag GmbH Germany, part of Springer Nature 2019

## Abstract

The Subei Shoal is a special coastal area with complex physical oceanographic properties in the Yellow Sea. In the present study, the distribution of phytoplankton and its correlation with environmental factors were studied during spring and summer of 2012 in the Subei Shoal of the Yellow Sea. Phytoplankton species composition and abundance data were accomplished by Utermöhl method. Diatoms represented the greatest cellular abundance during the study period. In spring, the phytoplankton cell abundance ranged from  $1.59 \times 10^3$  to  $269.78 \times 10^3$  cell/L with an average of  $41.80 \times 10^3$  cell/L, and *Skeletonema* sp. and *Paralia sulcata* was the most dominant species. In summer, the average phytoplankton cell abundance was  $72.59 \times 10^3$  cell/L with the range of  $1.78 \times 10^3$  to  $574.96 \times 10^3$  cell/L, and the main dominant species was *Pseudo-nitzschia pungens*, *Skeletonema* sp., *Dactylosolen fragilissima* and *Chaetoceros curvisetus*. The results of a redundancy analysis (RDA) showed that turbidity, temperature, salinity, pH, dissolved oxygen (DO), the ratio of dissolved inorganic nitrogen to silicate and  $\text{SiO}_4\text{-Si}$  (DIN/ $\text{SiO}_4\text{-Si}$ ) were the most important environmental factors controlling phytoplankton assemblages in spring or summer in the Subei Shoal of the Yellow Sea.

**Key words:** phytoplankton, Subei Shoal, eutrophication, turbidity, harmful algae blooms, Yellow Sea

**Citation:** Huo Yuanzi, Shi Honghua, Zhang Jianheng, Liu Qiao, Duan Yuanliang, He Qing, Yu Kefeng, Bi Hongsheng, Fan Chunlei, He Peimin. 2019. Spatio-temporal variability of phytoplankton assemblages and its controlling factors in spring and summer in the Subei Shoal of Yellow Sea, China. Acta Oceanologica Sinica, 38(10): 84–92, doi: 10.1007/s13131-019-1345-2

## 1 Introduction

The Yellow Sea is characterized by high loadings of sediment concentrations in the continental shelf regions (Guo and Yanagi, 1998; Shi and Wang, 2012). Sediment depositions from the ancient Huanghe River contributed to form the Subei Shoal off Jiangsu Province, China. This area gathers important urban centers as well as large industrial enterprises such as a petrochemical industrial park, a thermoelectric plant and fertilizer plants which make it economically important. This area is characterized by an extended shallow and muddy intertidal zone, which is up to 5 100 km<sup>2</sup>. These particular geographic conditions make it possible to construct harbors by extending bridge approaches into relatively deep-sea waters and are suitable for *Pyropia* aquaculture (Shang et al., 2008). The topographic characteristics and current patterns around the sand banks radiating off the Jiangsu coast are key factors that resulted in the famous fishing ground at

this area (Lu et al., 2002).

However, over the last few decades, the Subei Shoal has experienced high anthropogenic loadings of nutrients, particularly of dissolved inorganic nitrogen and phosphorus. The significantly eutrophication resulted in the reoccurrence of world's largest green macroalgae blooms since 2008 (Zhang et al., 2014a, 2017; Huo et al., 2013, 2016).

Phytoplankton is the main producers of organic matters in water bodies. The study of phytoplankton assemblages is the basis for understanding the mechanisms of ecosystem functioning in shelf seas. Up to now, extensive studies on qualitative and quantitative aspects of phytoplankton have been carried out in some coastal ecosystems in China (Shen et al., 2011; Liu et al., 2015a, b; Huo et al., 2018). However, knowledge on the dynamics of phytoplankton along the neighboring coastal system is rather poor, particularly in high turbulence waters.

Foundation item: The Public Science and Technology Research Funds Projects of the Ocean under contract Nos 201205010 and 201205009-5; the National Science & Technology Pillar Program under contract No. 2012BAC07B03; the National Natural Science Foundation of China under contract No. 41206111; the Chinese Science and Technology Base Projects under contract No. 2012FY112500; the Shanghai Universities First-class Disciplines Project (Disipline name: Marine Science (0707)); the Plateau Peak Disciplines Project of Shanghai Universities (Marine Science 0707).

\*Corresponding author, E-mail: [yzhuo@shou.edu.cn](mailto:yzhuo@shou.edu.cn)

Due to mesotidal conditions and circulation mechanisms, the Subei Shoal displays a very complex configuration. Seasonal monsoons, the coastal current, ocean fronts, and semidiurnal tides are primary processes that dominate the ocean hydrography in this area (Fang et al., 2004). The inner zone of Subei Shoal is highly turbid as a result of the combined effect of winds and tidal currents containing large amounts of suspended matters (Bian et al., 2013). The Subei Shoal is critical in view of the importance of this zone not only as a nursery area for several fish species (such as *Pseudosciaena polyactis*, *Isliha elongate*, *Setipinna tenuifilis* and *Pampus cinereus*) (Lopez Cazorla, 2000), but also as a natural reservation area, which is used as a multiple-use zone.

Understanding the biological processes forced by physical and chemical variability in the Subei Shoal is of fundamental importance to implement proper management strategies. Phytoplankton assemblages were studied by some researchers in the Yellow Sea (Liu et al., 2015a, b; Zhang et al., 2016), but very few documents were reported on the phytoplankton in the Subei Shoal of the Yellow Sea (Kang et al., 2013). Here we report spatial and temporal variations in the abundance and species composition of phytoplankton assemblages and their relationship with environmental variables in this area. The objectives of the present study were to identify the qualitative and quantitative abundance of phytoplankton and the influencing effects of environmental variables on phytoplankton species composition and their abundance, which would supply the fundamental data for understanding the ecological variations of Subei Shoal in the South Yellow Sea.

## 2 Materials and methods

### 2.1 Study area and survey methods

Most coastal waters of the Subei Shoal are located within the 20 m isobaths (Fig. 1). Two cruises were conducted in this area during the period from 8 to 14 in April (spring) and from 19 to 31 in August (summer) in 2012. Four transects (referred to as LS, RD, DF and BH), located in the Lvsi, Rudong, Dafeng and Binhai sea areas, respectively, were conducted for the purpose of environmental monitoring and to examine phytoplankton community (Fig. 1). Transects LS, RD and DF were conducted in April and Transects RD, DF and BH were conducted in August, respectively. During the period of this study, samples were collected from a total of 20 sampling sites. All transects extended to an approximate distance of 100 km offshore in the Yellow Sea.

### 2.2 Oceanographic conditions

During each survey, vertical temperature and salinity profiles were recorded at each sampling site, using a Sea-Bird (SBE 25) instrument lowered and retrieved from the sea surface to depths close to the sea bed. Seawater samples were collected at different water depths at each sampling site, using Niskin bottles, for the determination of ammonium ( $\text{NH}_4\text{-N}$ ), nitrite ( $\text{NO}_2\text{-N}$ ), nitrate nitrogen ( $\text{NO}_3\text{-N}$ ), soluble reactive phosphorus ( $\text{PO}_4\text{-P}$ ), soluble reactive silicate ( $\text{SiO}_4\text{-Si}$ ), total nitrogen (TN), total phosphorus (TP), and suspended sediment (SS) concentrations. Samples collected for the determination of dissolved inorganic nutrients were filtered through cellulose membranes ( $0.45\ \mu\text{m}$ ) which had been pre-immersed in 10% HCl for at least 10 h and rinsed with distilled water many times before use, after which a small amount of  $\text{HgCl}_2$  was added. A small amount of  $\text{H}_2\text{SO}_4$  was added to samples collected for TN and TP determinations, so as to bring the pH down to a level of less than 2.0. Seawater pH and

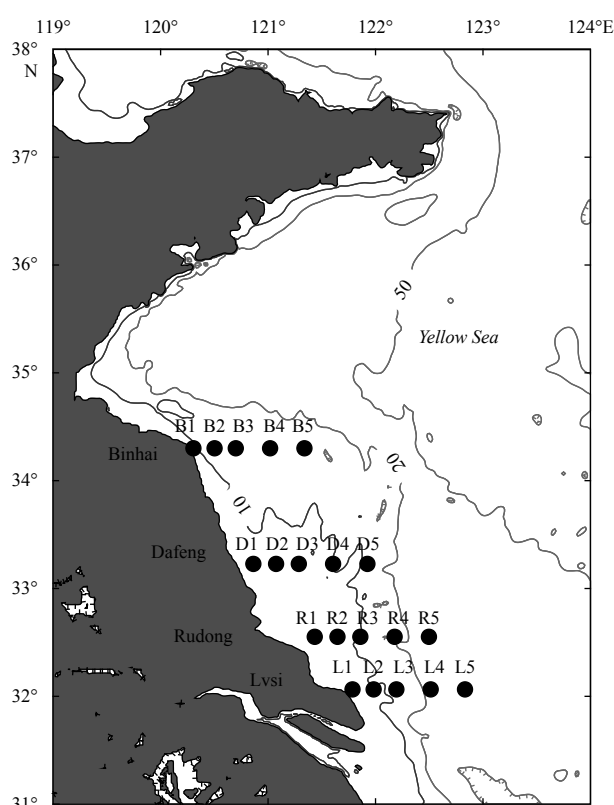


**Fig. 1.** Sampling transects along Lvsi (LS), Rudong (RD), Dafeng (DF) and Binhai (BH) and a total of 20 sampling sites along all transects at the southern coast of the Yellow Sea conducted in spring and summer of 2012.

turbidity were measured in the field, using a multi-parameter kit (MS5, HACH). Dissolved oxygen (DO) concentrations at different seawater depths were measured in the field, using the Winkler method. All seawater samples were transported to the laboratory under cold conditions, after which they were maintained at temperatures below  $-30^\circ\text{C}$ , until further analysis.

In the laboratory,  $\text{NH}_4\text{-N}$ ,  $\text{NO}_2\text{-N}$ ,  $\text{NO}_3\text{-N}$ ,  $\text{PO}_4\text{-P}$ , TN and TP concentrations were measured using a SKALAR flow analyzer (Breda, Netherlands). The  $\text{SiO}_4\text{-Si}$  concentration was determined by the standard molybdenum blue method. To determine suspended sediment (SS) concentrations, a certain volume of seawater was filtered through pre-weighed, pre-combusted ( $450^\circ\text{C}$ ) glass-fiber filters (Whatman GF/C), after which the filters were air-dried for 24–36 h in an oven at  $60^\circ\text{C}$  and weighed with an electronic balance.

### 2.3 Phytoplankton community structure

At each sampling site, 250 mL seawater was sampled at different depths using Niskin bottles, and these samples were immediately preserved with neutralized formaldehyde to a final concentration of 1%–2% for the determination of phytoplankton. Once the samples were taken back at the lab under cool conditions, they were settled in an Utermöhl counting chamber. Phytoplankton cells of greater than  $5\ \mu\text{m}$  diameter were identified and counted using an inverted microscope (Nikon Eclipse 100) at  $200\times$  and  $400\times$  magnification. The entire chamber was examined and each cell was counted as a unit. At least 400 individuals of the more abundant species were counted from each sample with a 10% error. Diatoms were identified to species level when possible. Iden-

tification keys used in this study are listed in Jin et al. (1965), Guo (2003), Zhang et al. (2016), Li et al. (2017), Wei et al. (2017), and in addition to Marshall (1994), Komárek and Anagnostidis (1986), Krammer and Lange-Bertalot (1991), and Tomas (1997). The dominance index ( $Y$ ) of the phytoplankton species, Shannon-Wiener diversity index ( $H'$ ), richness index ( $D$ ), and evenness index ( $J$ ) were calculated according Wang et al. (2005), Shannon and Weaver (1963), and Pielou (1975). A species with a  $Y > 0.02$  was considered as a dominant phytoplankton species in the present study.

#### 2.4 Statistical analysis

All data are displayed as mean  $\pm$  standard deviation/error. Based on the results of tests of normality, Pearson correlation analyses or Spearman correlation analyses were used to determine correlations between environmental factors and phytoplankton abundance. Statistical analyses were conducted using SPSS 19.0.

Multivariate ordination techniques were used to analyze the relationship of environmental variables with the phytoplankton community by CANOCO for Windows 4.5. The environmental parameters were adopted as the explanatory variables. All of these environmental parameters were transformed ( $\log_{10}x$ ) before analysis except for pH. In the data matrix of phytoplankton species abundance, only those species which was greater than 5% of the total abundance at least in one sample were used into the analysis. The phytoplankton species data were  $\log_{10}(x+1)$  transformed before analysis to obtain consecutive distributions. Detrended correspondence analysis (DCA) for the phytoplankton species data was employed to decide whether linear or unimodal ordination methods should be applied in this study. DCA revealed that the maximum gradient length of the four axes was lower than 3, therefore, redundancy analysis (RDA) was used, which was applied to assess the relationships between phytoplankton and environment parameters. Monte Carlo simulation was used to test the significance of the environmental parameters to explain the phytoplankton data in the RDA.

### 3 Results

#### 3.1 Environmental variables

During the study period, the spatio-temporal distribution of the environmental variables varied between the investigated two seasons. The results observed for these environmental variables were reported in Table 1 and Fig. 2 of the previous paper by Huo et al. (2014).

#### 3.2 Phytoplankton species composition

In spring, a total of 5 phyla, including 111 phytoplankton taxa belonging to 56 genera were detected during the study period,

and 53 species belonging to centric diatoms, 31 species belonging to pennate diatoms, 20 species belonging to dinoflagellates, 2 species belonging to Cyanophyta, 2 species belonging to Chlorophyta and 3 species belonging to Ochrophyta were identified. In August, a total of 5 phyla, including 136 phytoplankton taxa belonging to 61 genera were detected during the study period, and 79 species belonging to centric diatoms, 22 species belonging to pennate diatoms, 33 species belonging to dinoflagellates, 1 species belonging to Cyanophyta, 3 species belonging to Chlorophyta and 3 species belonging to Ochrophyta were identified. Diatoms dominated the phytoplankton assemblages at all sampling sites throughout the study period (Table 1).

#### 3.3 Phytoplankton cell abundance and spatial distribution

The average abundance of phytoplankton was  $41.80 \times 10^3$  cell/L with the range of  $1.59 \times 10^3$  to  $269.78 \times 10^3$  cell/L in spring, and was  $72.59 \times 10^3$  cell/L with the range of  $1.78 \times 10^3$  to  $574.96 \times 10^3$  cell/L in summer. Diatoms contributed the largest proportion to the total phytoplankton assemblage at all sampling sites throughout the observed period followed by dinoflagellates in both investigated seasons.

Spatial distribution of phytoplankton cell abundance in the surface water was shown in Fig. 2. In spring, the distribution of phytoplankton across sites was far from homogeneous. Highest densities of total phytoplankton cells were found in the inshore area along LS transaction. *Skeletonema* sp. was the most important species which accounted for 50.91% of total phytoplankton abundance throughout the observed period which mainly distributed in inshore area along LS transaction. *Thalassiosira leptopus* also mainly distributed in the inshore area on LS transaction. High cell abundance of *Planktoniella blanda* was observed at the open sea area on LS transaction. These four dominant species had low cell abundances along the DF and RD transaction. In summer, the highest phytoplankton cell abundance was found at the offshore area along the RD transaction. The distribution of diatoms was in accordance with the total phytoplankton abundance. High cell abundance of dinoflagellates was recorded at the open sea area along the BH transaction. *Pseudo-nitzschia pungens* and *Dactyliosolen fragilissima* mainly distributed at the open sea area along the RD transaction. The highest abundance of *Skeletonema* sp. was found at the sampling Site R3. The spatial distribution of dominant species shaped the distribution properties of total phytoplankton assemblages in both investigated seasons in this study period.

#### 3.4 Vertical distribution of phytoplankton cell abundance

The vertical distribution of phytoplankton cell abundance was showed in Fig. 3. In spring, the maximum cell abundance was recorded at the subsurface layer on all three transactions. The vertical distribution of phytoplankton was relatively homo-

**Table 1.** Dominant phytoplankton species in the Subei Shoal of the Yellow Sea in spring and summer in 2012

Season	Latin name	Frequency/%	Ratio of cell abundance/%	Dominance
Spring	<i>Skeletonema</i> sp.	87.5	50.91	0.445 5
	<i>Paralia sulcata</i>	95.0	20.61	0.195 8
	<i>Thalassiosira eccentrica</i>	100.0	3.78	0.037 8
	<i>Thalassiosira leptopus</i>	92.5	2.85	0.026 3
Summer	<i>Pseudo-nitzschia pungens</i>	80.5	27.33	0.220 0
	<i>Skeletonema</i> sp.	70.7	21.60	0.152 8
	<i>Dactyliosolen fragilissima</i>	61.0	12.14	0.074 0
	<i>Chaetoceros curvisetus</i>	24.4	14.80	0.036 1
	<i>Thalassionema frauenfeldii</i>	78.0	4.24	0.033 1

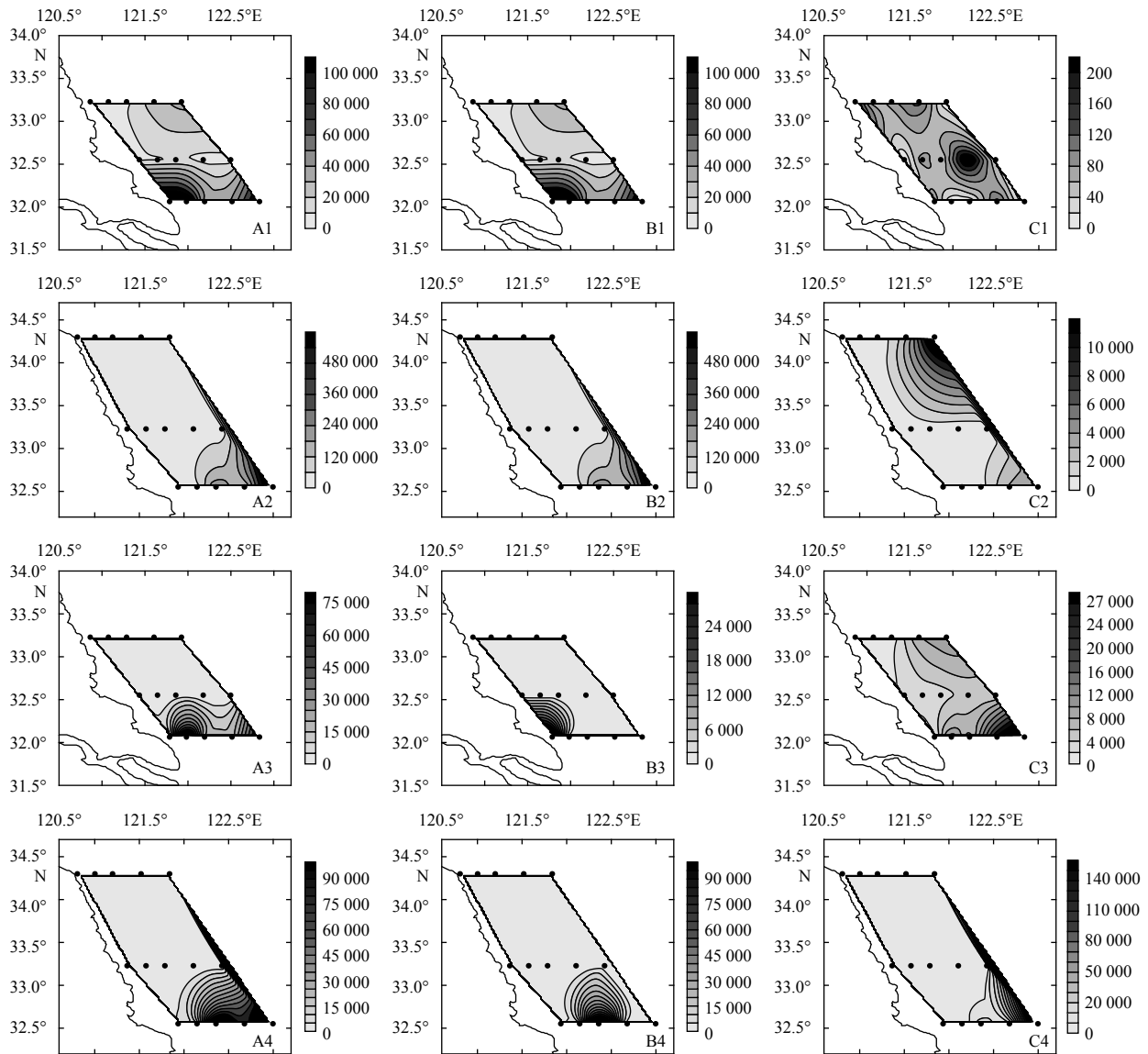


**Fig. 2.** The spatial distribution of the cell abundance (cell/L). A1, B1, C1 and A2, B2, C2 represent total phytoplankton, diatoms and dinoflagellates in spring and summer in 2012, respectively. A3, B3 and C3 represent *Skeletonema* sp., *Thalassiosira leptopus* and *Paralia sulcata* in spring. A4, B4 and C4 represent *Pseudo-nitzschia pungens*, *Skeletonema* sp. and *Dactyliosolen fragilissima* in summer.

geneous along the DF transaction at the open sea area. The total phytoplankton cell abundance was higher in the subsurface layer than the surface layer along the RD transaction. Relative high cell abundance was recorded at the subsurface layers along the LS transaction. *Skeletonema* sp. and *P. sulcata* prevailed three transects from the surface to the bottom, while *T. rotula* was the most abundant species at the inshore area of the DF transaction and *T. leptopus* was the most abundant species at the surface in the sampling Site L1.

In summer, the highest phytoplankton cell abundance was recorded at the subsurface layer along the BH and DF transaction. The relative high phytoplankton cell abundance attributed by *Gymnodinium* sp. was at the sea surface of offshore along the BH transaction. Along the RD transaction, high phytoplankton cell abundance was located at the surface layer of the open sea area, and *Chaetoceros curvisetus*, *Skeletonema* sp. and *P. pungens* prevailed in the whole water column of the inshore area.

### 3.5 Species diversity

Various biodiversity indexes can express the diversity of a phytoplankton community or assemblages in different ways, but the best way to evaluate the diversity of a community is using these indexes comprehensively (Sun and Liu, 2004). In this study, the values of Shannon-Wiener diversity index ( $H'$ ) and Pielou's evenness index ( $J$ ) showed a similar distribution patterns, and had always the opposite trends with phytoplankton cell abundance. The richness index ( $D$ ) was sensitive to dominance in both spring and summer. Shannon-Wiener diversity index of phytoplankton in spring ranged from 1.15 to 4.44 and the average value was 2.97. The phytoplankton cell abundance and diversity showed all high values in spring, which indicated that the phytoplankton assemblage was dominated by more species. Species richness and diversity of phytoplankton were higher in summer. Shannon-Wiener diversity index ranged from 0.72 to 4.37 and the average value was 3.00. Spatial distribution of Shannon-Wiener

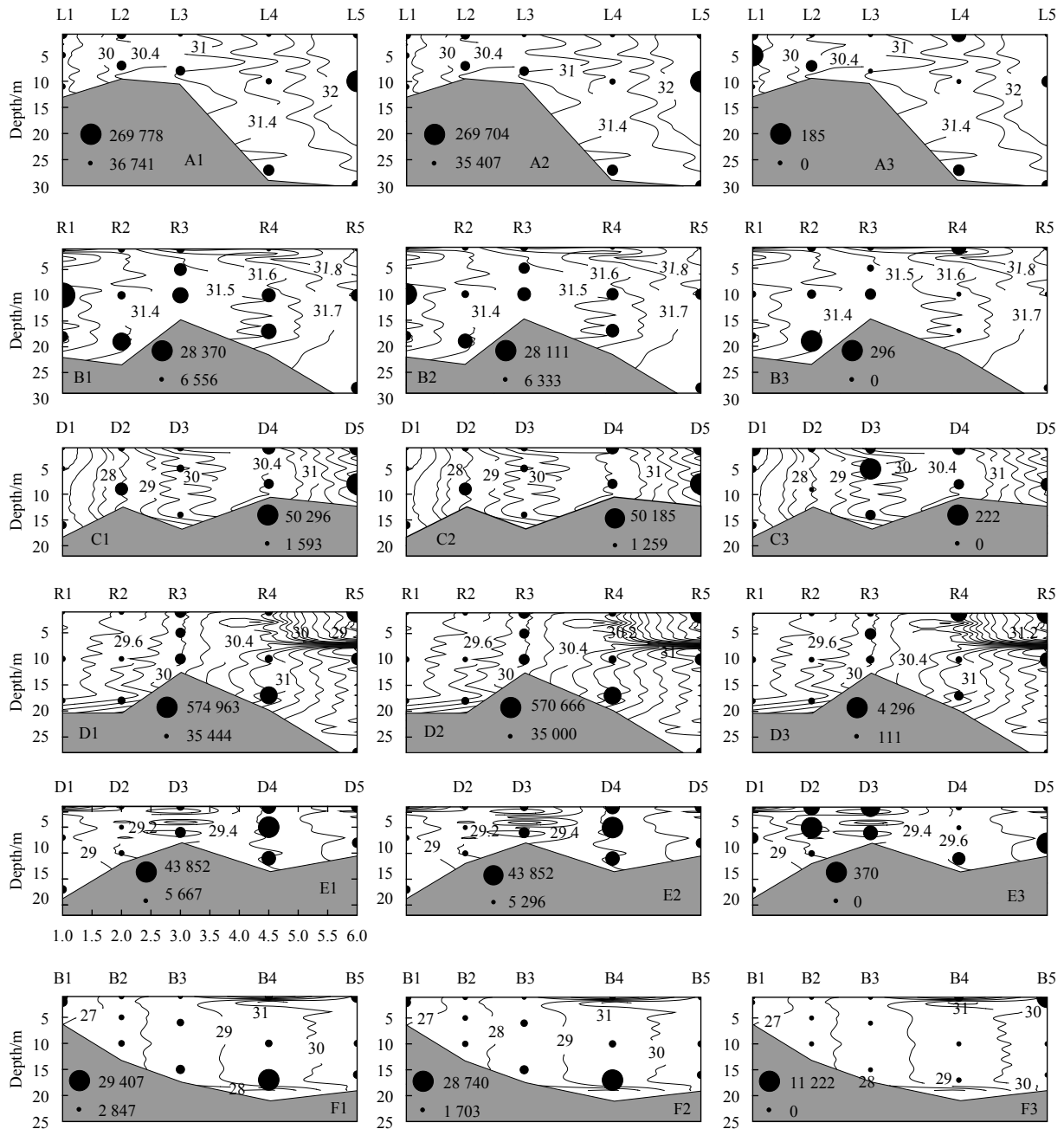


**Fig. 3.** The vertical distribution of cell abundance (cell/L, post map) and salinity (contour map). Total phytoplankton, diatoms and dinoflagellates was showed in A1, A2, A3, and B1, B2, B3, and C1, C2, C3 along the LS, RD, DF transaction in spring, and D1, D2, D3, and E1, E2, E3, and F1, F2, F3 along the RD, DF, BH transaction in summer, respectively.

diversity index showed greater values along the BH transaction and the inshore area of DF transaction than the other survey areas. The low diversity at the open sea area along the RD transaction indicated that the phytoplankton community was dominated by a few species, coinciding with the observed of high cell abundance of *P. pungens*, *Skeletonema* sp. and *D. fragilissima* during the sampling period in summer.

### 3.6 Relationships between phytoplankton and environmental variables

Pearson correlation analysis was used to explore the relationship between environment variables and phytoplankton composition at the time of sampling. The results indicate that  $\text{NH}_4\text{-N}$

and  $\text{NO}_2\text{-N}$  played important roles in the distribution of major phytoplankton species in spring (Table 2). Some individual species (e.g., *C. radiatus* and *P. blanda*) were associated with particular environmental variables, such as turbidity,  $\text{NO}_2\text{-N}$ . No significant relationship was found between the phytoplankton cell abundance and temperature, salinity in spring.  $\text{NH}_4\text{-N}$  and  $\text{NO}_2\text{-N}$  also played important roles in the distribution of major phytoplankton species in summer (Table 3). The dinoflagellate abundance was correlated with the lower nutrient conditions. In the case of salinity and temperature, *P. pungens* and *T. frauenfeldii* were associated with higher salinities and *T. frauenfeldii* was also negatively correlated with lower temperature.

The relationship between environmental factors and phyto-

**Table 2.** Pearson correlation between phytoplankton cell abundance and environmental factors in the Subei Shoal of the Yellow Sea in spring

	Temperature	Salinity	DO	TUR	NH <sub>4</sub> -N	NO <sub>2</sub> -N	NO <sub>3</sub> -N	PO <sub>4</sub> -P	SiO <sub>4</sub> -Si	TP
Total	-0.237	-0.245	-0.522**	-0.149	0.387*	0.535**	-0.119	0.015	0.038	0.022
Diatoms	-0.237	-0.244	-0.521**	-0.155	0.389*	0.527**	-0.122	0.012	0.035	0.019
Dinoflagellates	0.014	-0.034	0.081	-0.020	0.222	-0.069	0.050	0.009	-0.063	-0.156
<i>Skeletonema</i> sp.	-0.234	-0.263	-0.600**	0.115	0.147	0.558**	-0.028	0.072	0.128	0.293
<i>Paralia sulcata</i>	-0.223	-0.123	-0.273	-0.299	0.027	0.237	-0.574**	-0.232	-0.392*	-0.100
<i>Thalassiosira eccentrica</i>	-0.076	-0.050	0.060	0.341*	0.008	0.361*	-0.198	-0.030	-0.246	0.276
<i>Thalassiosira leptopus</i>	0.052	-0.003	-0.090	0.299	0.163	0.545**	0.126	0.291	0.082	0.195
<i>Coccinodiscus radiatus</i>	0.023	0.007	0.055	0.458**	0.074	0.445**	0.115	0.214	0.133	0.393*
<i>Planktoniella blanda</i>	0.002	-0.020	-0.164	0.404**	0.060	0.594**	-0.028	0.111	-0.015	0.384*
<i>Cylindrotheca closterium</i>	-0.135	-0.215	-0.230	0.456**	-0.101	0.486**	0.134	0.317*	0.042	0.319*
<i>Thalassiosira rotula</i>	0.059	-0.017	-0.225	0.194	0.069	0.043	0.067	0.304	-0.046	-0.058

Note: \* Correlation is significant at the 0.05 level (2-tailed); \*\* Correlation is significant at the 0.01 level (2-tailed). TUR represents turbidity.

**Table 3.** Pearson correlation between phytoplankton cell abundance and environmental factors in the Subei Shoal of the Yellow Sea in summer

	Temperature	Salinity	TUR	NH <sub>4</sub> -N	NO <sub>2</sub> -N	NO <sub>3</sub> -N	DIN	PO <sub>4</sub> -P	SiO <sub>4</sub> -Si
Total	-0.297	0.205	-0.369*	0.403**	0.400**	-0.386*	-0.265	-0.379*	-0.325*
Diatoms	-0.294	0.205	-0.368*	0.406**	0.400**	-0.383*	-0.261	-0.378*	-0.322*
Dinoflagellates	-0.220	0.099	-0.237	-0.029	0.087	-0.405**	-0.407**	-0.157	-0.386*
<i>Pseudo-nitzschia pungens</i>	-0.309	0.358*	-0.446	0.675**	0.533**	-0.463*	-0.284	-0.404*	-0.330
<i>Skeletonema</i> sp.	-0.246	0.287	-0.199	0.621**	0.374*	-0.273	-0.113	-0.212	-0.058
<i>Dactyliosolen fragilissima</i>	-0.197	-0.075	-0.249	-0.041	0.023	-0.216	-0.234	-0.365	-0.405*
<i>Chaetoceros curvisetus</i>	0.206	-0.660*	-0.258	-0.338	-0.300	-0.189	-0.610	-0.506	-0.865**
<i>Thalassionema frauenfeldii</i>	-0.360*	0.407*	-0.397*	0.551**	0.550**	-0.401*	-0.251	-0.188	-0.192

Note: \* Correlation is significant at the 0.05 level (2-tailed); \*\* Correlation is significant at the 0.01 level (2-tailed). TUR represents turbidity.

**Table 4.** Redundancy analysis results of phytoplankton in the Subei Shoal of the Yellow Sea in spring and summer in 2012

Axis	Eugeb value	Species–environment correlations	Cumulative percentage variance		Sum of all canonical eigenvalues
			Species	Species–environment relation	
Spring					
Axis 1	0.165	0.749	16.5	48.9	0.338
Axis 2	0.091	0.761	25.6	75.7	
Axis 3	0.054	0.743	31.0	91.6	
Axis 4	0.028	0.583	33.8	100	
Summer					
Axis 1	0.357	0.940	35.7	62.9	0.567
Axis 2	0.100	0.921	45.7	80.6	
Axis 3	0.052	0.744	50.9	89.8	
Axis 4	0.037	0.702	54.6	96.2	

plankton abundance was analyzed by RDA (Tables 4 and 5, Fig. 4). Monte Carlo tests for the first and all canonical axes were highly significant ( $p=0.002$ ) in two seasons, indicating that these parameters may be important in explaining phytoplankton community compositions. The first two axes explained 25.6% (spring) and 45.7% (summer) of the total variance in the phytoplankton abundance. Four significant canonical axes explained 33.8% and 54.6% of the phytoplankton variation during spring and summer, respectively. All canonical axes accounted for 33.8% of the variation in the phytoplankton data during spring, and 56.7% during summer (Table 4).

There were different significant environmental variables explaining the variability in the phytoplankton composition during

two seasons by RDA with forward selection (Table 5, Fig. 4). During spring, turbidity, salinity, SiO<sub>4</sub>-Si and temperature were found to statistically explain the variation in the composition of phytoplankton. However, during summer, the significant environmental variables were turbidity, temperature, DO, DIN/SiO<sub>4</sub>-Si, SiO<sub>4</sub>-Si, and pH.

#### 4 Discussion

The topography of the Subei Shoal constrains the features of the currents and causes net longitudinal and latitudinal movements (Bao et al., 2015), and this area was also strongly affected by runoff from nearby rivers and human activities, which causes the specific characteristics of the current, the temperature, the

**Table 5.** Variation partitioning analysis of the significant environmental factors on the phytoplankton assemblages in the Subei Shoal of Yellow Sea in spring and summer in 2012

Environmental factor	Eigenvalues	Variation explains solely/%	F	p
Spring				
Turbidity	0.099	9.9	4.152	0.002
Salinity	0.103	10.3	4.795	0.002
SiO <sub>4</sub> -Si	0.073	7.3	3.636	0.004
Temperature	0.063	6.3	3.326	0.002
All the above together	0.338	33.8	4.326	0.002
Summer				
Turbidity	0.279	27.9	15.059	0.002
Temperature	0.09	9.0	5.384	0.002
DO	0.069	6.9	4.551	0.002
N/Si	0.06	6.0	4.272	0.002
SiO <sub>4</sub> -Si	0.041	4.1	3.074	0.002
pH	0.029	2.9	2.300	0.008
All the above together	0.568	56.8	7.362	0.002

salinity, the nutrient structures and suspended particulate matters (SPMs) in seawaters (Huo et al., 2013), e.g., the 140 mg/dm<sup>3</sup> of the three-month-averaged surface SPM (April, May and June) in the Subei Shoal (Bao et al., 2015). Sediment transport processes also play a critical role in shaping the ecological environment and the material exchange between the inner shelf and the outer seas, e.g., highest concentrations of suspended sediment in the Subei Shoal (Bian et al., 2013). The gradients of environmental factors seaward strongly influence the species composition, distribution and abundance of biological communities.

Both seasonal and spatial variations of phytoplankton community were observed in the Subei Shoal. The phytoplankton composition in the Subei Shoal was characteristic by diatoms dominated during both seasons, contributing up to 98.5% and 98.6% of total abundance in spring and summer, respectively, which was in accordance with the results reported by Liu et al. (2015a) who indicated that diatoms contributed 98% of the Chl *a* concentration to the water column in April at the offshore of South Yellow Sea, but the average concentration and relative abundance of diatoms in the central area were only 0.05 mg/m<sup>3</sup> and 30%, when the Yellow Sea Cold Water Mass (YSCWM) prevailed during their August cruise. In the present study, the phytoplankton species composition and cell abundance were significantly different between two seasons, and the total taxa and cell abundance were higher in summer than those in spring. *Skeletonema* sp. was the dominant species in both spring and summer. *Thalassiosira pacifica*, *Guinardia delicatula* and *Corethron pennatum* dominated the spring bloom in the South Yellow Sea in April (Liu et al., 2015a), which was not the dominant species in the Subei Shoal during the same investigated period. And *Pseudo-nitzschia delicatissima* was only the same dominant species compared with our results in summer (June) reported by Liu et al. (2015b) at the offshore areas of South Yellow Sea. In this study, the total cell abundance and dominant species were higher at the Subei Shoal area than those at the offshore of South Yellow Sea during the same investigated seasons (Liu et al., 2015a, b). The sampling location in the Subei Shoal conducted by Kang et al. (2013) was different with the sampling location in the present study. The total cell abundance reported by Kang et al. (2013) was higher than that compared with the present study in spring. The results of present study indicated that the phyto-

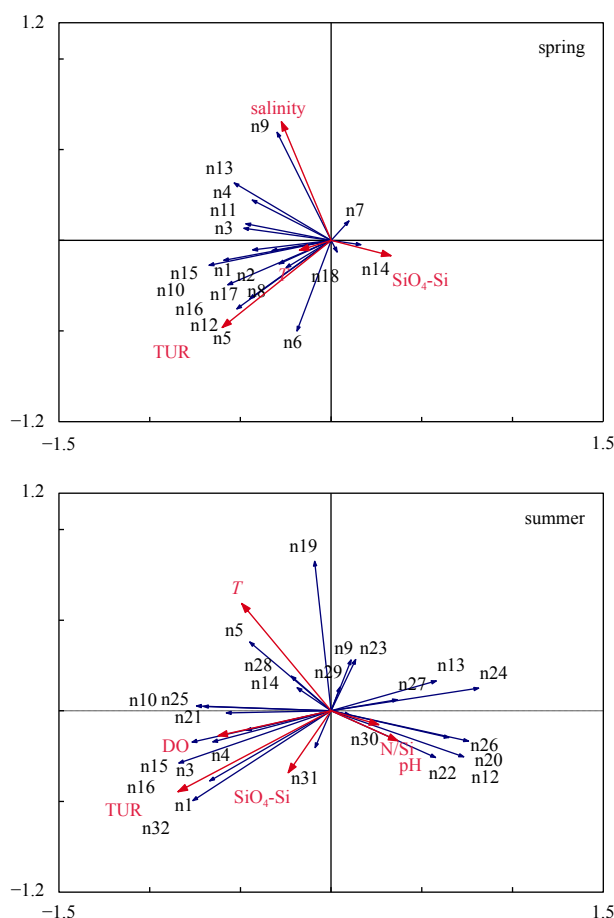


**Fig. 4.** Correlation plots of the redundancy analysis (RDA) for the relationship between the environmental variables and phytoplankton taxa. *T* represents water temperature and *TUR* turbidity. The numbers with letters represent the following species: n1 represents *Actinopterychus senarius*, n2 *Bacillaria paxillifera*, n3 *Coscinodiscus radiatus*, n4 *Coscinodiscus* sp., n5 *Cylindrotheca closterium*, n6 *Fragillariopsis* sp., n7 *Navicula* sp., n8 *Nitzschia* sp., n9 *Paralia sulcata*, n10 *Planktoniella blanda*, n11 *Pleurosigma* sp., n12 *Pseudo-nitzschia pungens*, n13 *Skeletonema* sp., n14 *Thalassionema nitzschioides*, n15 *Thalassiosira eccentrica*, n16 *Thalassiosira leptopus*, n17 *Thalassiosira rotula*, n18 *Scenedesmus quadricauda*, n19 *Campylosira cymbelliformis*, n20 *Chaetoceros curvisetus*, n21 *Coscinodiscus jonesianus*, n22 *Dactyliosolen fragillissima*, n23 *Melosira nummuloides*, n24 *Pseudo-nitzschia delicatissima*, n25 *Surirella* sp., n26 *Thalassionema frauenfeldii*, n27 *Thalassiosira* sp., n28 *Thalassiosira subtilis*, n29 *Alexandrium catenella*, n30 *Gymnodinium* sp., n31 *Pediastrum duplex*, and n32 *Dictyocha fibula*.

plankton species composition and cell abundance were completely different between the Subei Shoal and the offshore of Yellow Sea in both spring and summer.

A key part of determining the productive capacities of the temperate continental shelf is to understand the temporal and spatial dynamics of its prevailing phytoplankton taxonomic groups (Chang et al., 2003). The species composition during each season was dominated by different species. During spring, phytoplankton assemblages mainly composed by centric diatoms such as *Skeletonema* sp., *P. sulcata* and *T. eccentrica*, while a pennate species *P. pungens* became the most important species, and fol-

lowed by *Skeletonema* sp. during summer. In the different oceanographic zones of the Subei Shoal, phytoplankton communities varied throughout the spring and summer with regard to cell concentration, species composition and distribution pattern. The offshore investigated region of Subei Shoal was characterized by stable salinities and relatively high light availability (Huo et al., 2013, 2014). The phytoplankton abundance were much greater in upper estuary than those of mixing and ocean regions, reflecting the influence of freshwater discharge from the Changjiang River (Yangtze River). The results of present study also showed that the abundance of total phytoplankton and dominant species were most distributed at the offshore area and near the Changjiang Estuary in the Subei Shoal.

The seasonal variations of the phytoplankton community and their abundance were greatly influenced by environmental factors (Peng et al., 2012). In the present study, the most important environmental factors were water temperature, salinity, turbidity, and nutrients. Water temperature can control the seasonal dynamics of phytoplankton successions (Dupuis and Hann, 2009). The abundance of diatoms is inversely related to temperature, and a high abundance of diatoms was at temperatures below 18°C (da Silva et al., 2005; Turner et al., 2009). In the Subei Shoal, the total diatom abundance was all high in spring and summer, which differs from those in the Bohai Bay (Peng et al., 2012). The abundance of small-celled diatoms, such as *Skeletonema* sp., increases during warm water periods, because warm water is well known to be less viscous than cold water, favoring a species with a small cell size (Tunin-Ley et al., 2007).

Nutrient availability is one of key factors influencing the variations of the phytoplankton community (Lope et al., 2009; Ward et al., 2011; Huo et al., 2018). Under normal conditions, phytoplankton takes up N and P at the Redfield ratio (16:1). In the Subei Shoal, the observed molar ratio of N/P was higher than the Redfield ratio, and there was no significant correlation between phytoplankton abundance and the PO<sub>4</sub>-P concentration, which indicated that phytoplankton abundance was not limited by PO<sub>4</sub>-P availability during the study period. During the study period, the phytoplankton community was dominated by diatom species in the Subei Shoal. The concentration of SiO<sub>4</sub>-Si could influence the structure of phytoplankton assemblages, with diatoms becoming the dominant species when the SiO<sub>4</sub>-Si concentration was higher than 2 μmol/L and the levels of all other nutrients were sufficient (Egge, 1998). *Skeletonema* sp. dominated the phytoplankton community during spring and summer, suggesting that *Skeletonema* sp. prefers water with high levels of nutrients (Patil and Anil, 2011; Peng et al., 2012). *Cylindrotheca closterium* and *P. sulcata* also have a preference for seawater containing high nutrient concentrations (Du et al., 2016; El-Kassas and Gharib, 2016; Zhang et al., 2016). *Pseudo-nitzschia delicatissima* was one of the dominant species in the summer, and is considered to be an estuarine species that is typically observed in the high flow season, which is characterized by a relatively high salinity (Zhang et al., 2014b). In the RDA with forward selection, the abundance of *P. sulcata*, *P. pungens*, *T. frauenfeldii*, *C. radiatus*, *Coscinodiscus* sp. and other species had a strong correlation with pH, dissolved oxygen and salinity in spring or summer investigated in the Subei Shoal, which was consistent with the results reported by Rai and Rajashekar (2014).

High turbidity is one of the important characteristics in the Subei Shoal of South Yellow Sea. The Subei Shoal had the highest suspended sediment concentrations in all four seasons (Bian et al., 2013). The Changjiang River Plume can also increase the water turbidity at the coast nearby the river estuary. In general, the

relatively high suspended matter or high phytoplankton population are responsible for relatively high turbidity that is encountered in coastal waters. Fan et al. (2016) reported that high concentrations of suspended particulate material (SPM) in the surface layer located on the Subei Shoal and off the Changjiang Estuary overlap with the high Chl *a* concentration, and in the surface layer, the main part of small SPMs is composed of phytoplankton, whereas large SPMs are primarily dominated by mesozooplankton. In the present study, several phytoplankton species, such as *C. closterium*, *Nitzschia* sp., *P. pungens*, *A. senarius*, *T. leptopus*, *D. fibula*, had strongly correlations with the turbidity during the study period in both spring and summer.

In summary, diatoms represented the greatest cellular abundance in the Subei Shoal during spring and summer, and *Skeletonema* sp. and *P. pungens* was the most abundant species. The phytoplankton composition and abundance in the Subei Shoal was different compared with the offshore area of Yellow Sea according to previous studies in spring and summer. Turbidity, temperature, salinity, pH, DO, DIN/SiO<sub>4</sub>-Si and SiO<sub>4</sub>-Si were the most important environmental factors controlling phytoplankton assemblages in spring or summer seasons in the Subei Shoal of Yellow Sea. The results of present study supplied the fundamental data to understand variations of the Subei Shoal ecosystem.

#### Acknowledgements

We thank the crew of the R/V *Maritime Surveillance 59* for their assistance in the field.

#### References

- Bao Min, Guan Weibing, Wang Zongling, et al. 2015. Features of the physical environment associated with green tide in the southwestern Yellow Sea during spring. *Acta Oceanologica Sinica*, 34(7): 97–104, doi: [10.1007/s13131-015-0692-x](https://doi.org/10.1007/s13131-015-0692-x)
- Bian Changwei, Jiang Wensheng, Quan Qi, et al. 2013. Distributions of suspended sediment concentration in the Yellow Sea and the East China Sea based on field surveys during the four seasons of 2011. *Journal of Marine Systems*, 121–122: 24–35, doi: [10.1016/j.jmarsys.2013.03.013](https://doi.org/10.1016/j.jmarsys.2013.03.013)
- Chang F H, Zeldis J, Gall M, et al. 2003. Seasonal and spatial variation of phytoplankton assemblages, biomass and cell size from spring to summer across the north-eastern New Zealand continental shelf. *Journal of Plankton Research*, 25(7): 737–758, doi: [10.1093/plankt/25.7.737](https://doi.org/10.1093/plankt/25.7.737)
- da Silva C A, Train S, Rodrigues L C. 2005. Phytoplankton assemblages in a Brazilian subtropical cascading reservoir system. *Hydrobiologia*, 537(1–3): 99–109, doi: [10.1007/s10750-004-2552-0](https://doi.org/10.1007/s10750-004-2552-0)
- Du Guoying, Chung I K, Xu Henglong. 2016. Insights into community-based bioassessment of environmental quality status using microphytobenthos in estuarine intertidal ecosystems. *Acta Oceanologica Sinica*, 35(6): 112–120, doi: [10.1007/s13131-016-0874-1](https://doi.org/10.1007/s13131-016-0874-1)
- Dupuis A P, Hann B J. 2009. Warm spring and summer water temperatures in small eutrophic lakes of the Canadian prairies: potential implications for phytoplankton and zooplankton. *Journal of Plankton Research*, 31(5): 489–502, doi: [10.1093/plankt/fbp001](https://doi.org/10.1093/plankt/fbp001)
- Egge J K. 1998. Are diatoms poor competitors at low phosphate concentrations?. *Journal of Marine Systems*, 16(3–4): 191–198, doi: [10.1016/S0924-7963\(97\)00113-9](https://doi.org/10.1016/S0924-7963(97)00113-9)
- El-Kassas H Y, Gharib S M. 2016. Phytoplankton abundance and structure as indicator of water quality in the drainage system of the Burullus Lagoon, southern Mediterranean coast, Egypt. *Environmental Monitoring and Assessment*, 188(9): 530, doi: [10.1007/s10661-016-5525-7](https://doi.org/10.1007/s10661-016-5525-7)
- Fan Renfu, Wei Hao, Zhao Liang. 2016. Linking suspended particulate material characteristics to the plankton distribution in summer in the Yellow Sea and East China Sea. *Journal of*

- Coastal Research, 32(4): 829–839
- Fang Guohong, Wang Yonggang, Wei Zexun, et al. 2004. Empirical cotidal charts of the Bohai, Yellow, and East China Seas from 10 years of TOPEX/Poseidon altimetry. *Journal of Geophysical Research*, 109: C11006, doi: [10.1029/2004JC002484](https://doi.org/10.1029/2004JC002484)
- Guo Yujie. 2003. *Flora Algarum Marinarum Sinicarum*. Tomus V. Bacillariophyta, No. 1, Centricae (in Chinese). Beijing: Science Press, 1–493
- Guo Xinyu, Yanagi T. 1998. Three-dimensional structure of tidal current in the East China Sea and the Yellow Sea. *Journal of Oceanography*, 54(6): 651–668, doi: [10.1007/BF02823285](https://doi.org/10.1007/BF02823285)
- Huo Yuanzi, Han Hongbin, Hua Liang, et al. 2016. Tracing the origin of green macroalgal blooms based on the large scale spatio-temporal distribution of *Ulva* microscopic propagules and settled mature *Ulva* vegetative thalli in coastal regions of the Yellow Sea, China. *Harmful Algae*, 59: 91–99, doi: [10.1016/j.hal.2016.09.005](https://doi.org/10.1016/j.hal.2016.09.005)
- Huo Yuanzi, Hua Liang, Wu Hailong, et al. 2014. Abundance and distribution of *Ulva* microscopic propagules associated with a green tide in the southern coast of the Yellow Sea. *Harmful Algae*, 39: 357–364, doi: [10.1016/j.hal.2014.09.008](https://doi.org/10.1016/j.hal.2014.09.008)
- Huo Yuanzi, Zhang Jianheng, Chen Liping, et al. 2013. Green algae blooms caused by *Ulva prolifera* in the southern Yellow Sea: Identification of the original bloom location and evaluation of biological processes occurring during the early northward floating period. *Limnology and Oceanography*, 58(6): 2206–2218, doi: [10.4319/lo.2013.58.6.2206](https://doi.org/10.4319/lo.2013.58.6.2206)
- Huo Yuanzi, Wei Zhangliang, Liu Qiao, et al. 2018. Distribution and controlling factors of phytoplankton assemblages associated with mariculture in an eutrophic enclosed bay in the East China Sea. *Acta Oceanologica Sinica*, 37(8): 102–112, doi: [10.1007/s13131-018-1238-9](https://doi.org/10.1007/s13131-018-1238-9)
- Jin Dexiang, Chen Jinhuan, Huang Kaige. 1965. *Marine Planktonic Diatoms of China Seas* (in Chinese). Shanghai: Shanghai Scientific and Technical Publishers, 1–230
- Kang Wei, Sun Yue, Sun Lufeng, et al. 2013. Distribution of phytoplankton in radial sand ridge area in north Jiangsu Shoal. *Chinese Journal Applied Environmental Biology* (in Chinese), 19(5): 727–733, doi: [10.3724/SP.J.1145.2013.00727](https://doi.org/10.3724/SP.J.1145.2013.00727)
- Komárek J A, Anagnostidis K. 1986. Modern approach to the classification systems of cyanophytes 2-Chroococales. *Archiv für Hydrobiologie Supplementband*, 73: 157–226
- Krammer K, Lange-Bertalot H. 1991. *Süßwasserflora von Mitteleuropa*. Bd 2/3: Bacillariophyceae 3. Teil: Centrales, Fragilariaceae, Eunotiaceae. Stuttgart: Gustav Fischer Verlag, 1–576
- Li Xiaojian, Feng Yuanyuan, Leng Xiaoyun, et al. 2017. Phytoplankton species composition of four ecological provinces in Yellow Sea, China. *Journal of Ocean University of China*, 16(6): 1115–1125, doi: [10.1007/s11802-017-3270-3](https://doi.org/10.1007/s11802-017-3270-3)
- Liu Xin, Huang Bangqin, Huang Qiu, et al. 2015a. Seasonal phytoplankton response to physical processes in the southern Yellow Sea. *Journal of Sea Research*, 95: 45–55, doi: [10.1016/j.seares.2014.10.017](https://doi.org/10.1016/j.seares.2014.10.017)
- Liu Haijiao, Huang Yajie, Zhai Weidong, et al. 2015b. Phytoplankton communities and its controlling factors in summer and autumn in the southern Yellow Sea, China. *Acta Oceanologica Sinica*, 34(2): 114–123, doi: [10.1007/s13131-015-0620-0](https://doi.org/10.1007/s13131-015-0620-0)
- Lope M, Chan K S, Ciannelli L, et al. 2009. Effects of environmental conditions on the seasonal distribution of phytoplankton biomass in the North Sea. *Limnology and Oceanography*, 54(2): 512–524, doi: [10.4319/lo.2009.54.2.0512](https://doi.org/10.4319/lo.2009.54.2.0512)
- Lopez C A. 2000. Age structure of the population of weakfish *Cynoscion guatucupa* (Cuvier) in the Bahía Blanca waters, Argentina. *Fisheries Research*, 46(1–3): 279–286, doi: [10.1016/S0165-7836\(00\)00152-1](https://doi.org/10.1016/S0165-7836(00)00152-1)
- Liu Liyun, Zhang Renshun, Chen Jun. 2002. The developing and utilizing foreground of Jiangsu coastal radiate sandbands. *Journal of Nanjing Normal University* (Natural Science Edition) (in Chinese), 25(3): 18–24
- Marshall H G. 1994. Chesapeake bay phytoplankton: I. Composition. *Proceedings of the Biological Society of Washington*, 107: 573–585
- Patil J S, Anil A C. 2011. Variations in phytoplankton community in a monsoon influenced tropical estuary. *Environmental Monitoring and Assessment*, 182(1–4): 291–300, doi: [10.1007/s10661-011-1876-2](https://doi.org/10.1007/s10661-011-1876-2)
- Peng Shitao, Qin Xuebo, Shi Honghua, et al. 2012. Distribution and controlling factors of phytoplankton assemblages in a semi-enclosed bay during spring and summer. *Marine Pollution Bulletin*, 64(5): 941–948, doi: [10.1016/j.marpolbul.2012.03.004](https://doi.org/10.1016/j.marpolbul.2012.03.004)
- Pielou E C. 1975. *Ecological Diversity*. New York: Wiley, 16–51
- Rai S V, Rajashekhar M. 2014. Seasonal assessment of hydrographic variables and phytoplankton community in the Arabian sea waters of Kerala, Southwest coast of India. *Brazilian Journal of Oceanography*, 62(4): 279–289, doi: [10.1590/s1679-87592014069906204](https://doi.org/10.1590/s1679-87592014069906204)
- Shang Zhaotang, Jiang Mingshu, Pu Meijuan. 2008. Analysis of the general situations of Laver culture in Jiangsu province and its climatic suitability. *Journal of Anhui Agricultural Sciences* (in Chinese), 36(13): 5315–5319
- Shannon C E, Weaver W. 1963. *The Mathematical Theory of Communication*. Urbana: University of Illinois Press, 1–117
- Shen Pingping, Li Gang, Huang Liangmin, et al. 2011. Spatio-temporal variability of phytoplankton assemblages in the Pearl River estuary, with special reference to the influence of turbidity and temperature. *Continental Shelf Research*, 31(16): 1672–1681, doi: [10.1016/j.csr.2011.07.002](https://doi.org/10.1016/j.csr.2011.07.002)
- Shi Wei, Wang Menghua. 2012. Satellite views of the Bohai Sea, Yellow Sea, and East China Sea. *Progress in Oceanography*, 104: 30–45, doi: [10.1016/j.pocean.2012.05.001](https://doi.org/10.1016/j.pocean.2012.05.001)
- Sun Jun, Liu Dongyan. 2004. The application of diversity indices in marine phytoplankton studies. *Haiyang Xuebao* (In Chinese), 26(1): 62–75
- Tomas C R. 1997. *Identifying Marine Phytoplankton*. San Diego: Academic Press, 1–858
- Tunin-Ley A, Labat J P, Gasparini S, et al. 2007. Annual cycle and diversity of species and infraspecific taxa of *Ceratium* (Dinophyceae) in the Ligurian sea, northwest Mediterranean. *Journal of Phycology*, 43(6): 1149–1163, doi: [10.1111/jpy.2007.43.issue-6](https://doi.org/10.1111/jpy.2007.43.issue-6)
- Turner J W, Good B, Cole D, et al. 2009. Plankton composition and environmental factors contribute to *Vibrio* seasonality. *ISME J*, 3(9): 1082–1092, doi: [10.1038/ismej.2009.50](https://doi.org/10.1038/ismej.2009.50)
- Wang Yunlong, Yuan Qi, Shen Xinqiang. 2005. Ecological character of phytoplankton in spring in the Yangtze River estuary and adjacent waters. *Journal of Fishery Sciences of China* (in Chinese), 12(3): 300–306
- Ward B B, Rees A P, Somerfield P J, et al. 2011. Linking phytoplankton community composition to seasonal changes in f-ratio. *ISME J*, 5(11): 1759–1770, doi: [10.1038/ismej.2011.50](https://doi.org/10.1038/ismej.2011.50)
- Wei Yuqiu, Liu Haijiao, Zhang Xiaodong, et al. 2017. Physicochemical conditions in affecting the distribution of spring phytoplankton community. *Chinese Journal of Oceanology and Limnology*, 35(6): 1342–1361, doi: [10.1007/s00343-017-6190-6](https://doi.org/10.1007/s00343-017-6190-6)
- Zhang Jianheng, Huo Yuanzi, Wu Hailong, et al. 2014a. The origin of the *Ulva* macroalgal blooms in the Yellow Sea in 2013. *Marine Pollution Bulletin*, 89(1–2): 276–283, doi: [10.1016/j.marpolbul.2014.09.049](https://doi.org/10.1016/j.marpolbul.2014.09.049)
- Zhang Shan, Leng Xiaoyun, Feng Yuanyuan, et al. 2016. Ecological provinces of spring phytoplankton in the Yellow Sea: species composition. *Acta Oceanologica Sinica*, 35(8): 114–125, doi: [10.1007/s13131-016-0872-3](https://doi.org/10.1007/s13131-016-0872-3)
- Zhang Xia, Zhang Jingping, Huang Xiaoping, et al. 2014b. Phytoplankton assemblage structure shaped by key environmental variables in the Pearl River Estuary, South China. *Journal of Ocean University of China*, 13(1): 73–82, doi: [10.1007/s11802-014-1972-3](https://doi.org/10.1007/s11802-014-1972-3)
- Zhang Jianheng, Zhao Peng, Huo Yuanzi, et al. 2017. The fast expansion of *Pyropia* aquaculture in “Sansha” regions should be mainly responsible for the *Ulva* blooms in Yellow Sea. *Estuarine, Coastal and Shelf Science*, 189: 58–65, doi: [10.1016/j.ecss.2017.03.011](https://doi.org/10.1016/j.ecss.2017.03.011)